JOURNAL OF PROTEOMICS 99 (2014) 68–83

Available online at www.sciencedirect.com

ScienceDirect

www.elsevier.com/locate/jprot

Intraspecific venom variation in the medically significant Southern Pacific Rattlesnake (*Crotalus oreganus helleri*): Biodiscovery, clinical and evolutionary implications

Kartik Sunagar[a,b,1], *Eivind A.B. Undheim*[c,d,1], *Holger Scheib*[d,1], *Eric C.K. Gren*[e,1], *Chip Cochran*[e,1], *Carl E. Person*[e,1], *Ivan Koludarov*[c], *Wayne Kelln*[e], *William K. Hayes*[e], *Glenn F. King*[d], *Agosthino Antunes*[a,b], *Bryan Grieg Fry*[c,d,*]

[a]*Departamento de Biologia, Faculdade de Ciências, Universidade do Porto, Rua do Campo Alegre, 4169-007 Porto, Portugal*
[b]*CIIMAR/CIMAR, Interdisciplinary Centre of Marine and Environmental Research, University of Porto, Rua dos Bragas 289, P 4050-123 Porto, Portugal*
[c]*Venom Evolution Lab, School of Biological Sciences, University of Queensland, St. Lucia, Queensland, Australia*
[d]*Institute for Molecular Bioscience, University of Queensland, St. Lucia, Queensland 4072, Australia*
[e]*Department of Earth and Biological Sciences, Loma Linda University, Loma Linda, CA 92350, USA*

ARTICLE INFO

Article history:
Received 6 September 2013
Accepted 13 January 2014

Keywords:
Venom
Evolution
Molecule
Toxin
Rattlesnake
Crotalus

ABSTRACT

Due to the extreme variation of venom, which consequently results in drastically variable degrees of neutralization by CroFab antivenom, the management and treatment of envenoming by *Crotalus oreganus helleri* (the Southern Pacific Rattlesnake), one of the most medically significant snake species in all of North America, has been a clinician's nightmare. This snake has also been the subject of sensational news stories regarding supposed rapid (within the last few decades) evolution of its venom. This research demonstrates for the first time that variable evolutionary selection pressures sculpt the intraspecific molecular diversity of venom components in *C. o. helleri*. We show that myotoxic β-defensin peptides (aka: crotamines/small basic myotoxic peptides) are secreted in large amounts by all populations. However, the mature toxin-encoding nucleotide regions evolve under the constraints of negative selection, likely as a result of their non-specific mode of action which doesn't enforce them to follow the regime of the classic predator–prey chemical arms race. The hemorrhagic and tissue destroying snake venom metalloproteinases (SVMPs) were secreted in larger amounts by the Catalina Island and Phelan rattlesnake populations, in moderate amounts in the Loma Linda population and in only trace levels by the Idyllwild population. Only the Idyllwild population in the San Jacinto Mountains contained potent presynaptic neurotoxic phospholipase A_2 complex characteristic of Mohave Rattlesnake (*Crotalus scutulatus*) and Neotropical Rattlesnake (*Crotalus durissus terrificus*). The derived heterodimeric lectin toxins characteristic of viper venoms, which exhibit a diversity of biological activities, including anticoagulation, agonism/antagonism of platelet activation, or procoagulation, appear to have evolved under extremely variable selection pressures. While most lectin α- and β-chains evolved rapidly under the influence of positive Darwinian selection, the β-chain lectin of the

* *Corresponding author at:* Venom Evolution Lab, School of Biological Sciences, University of Queensland, St. Lucia, Queensland, Australia. E-mail address: bgfry@uq.edu.au (B.G. Fry).
[1] Joint first-author.

http://dx.doi.org/10.1016/j.jprot.2014.01.013

Catalina Island population appears to have evolved under the constraint of negative selection. Both lectin chains were conspicuously absent in both the proteomics and transcriptomics of the Idyllwild population. Thus, we not only highlight the tremendous biochemical diversity in *C. o. helleri*'s venom-arsenal, but we also show that they experience remarkably variable strengths of evolutionary selection pressures, within each toxin class among populations and among toxin classes within each population. The mapping of geographical venom variation not only provides additional information regarding venom evolution, but also has direct medical implications by allowing prediction of the clinical effects of rattlesnake bites from different regions. Such information, however, also points to these highly variable venoms as being a rich source of novel toxins which may ultimately prove to be useful in drug design and development.

Biological significance

- These results have direct implications for the treatment of envenomed patients.
- The variable venom profile of *Crotalus oreganus helleri* underscores the biodiscovery potential of novel snake venoms.

1. Introduction

Knowledge of venom composition has increased dramatically with improvements in technology and the advent of new techniques, in particular the use of mass spectrometry in venom proteomics [1–15] and venom gland transcriptome analysis [16–27]. Snake venoms are complex secretions composed of numerous enzymes, toxins, peptides, small organic molecules, and inorganic components that have diverse modes of action on both prey and human victims [28–32]. Snake venom serves both predatory and defensive purposes [28–30,33–38]. Variation in venom profiles has been shown between species within the same genus [5,11,12,15,27,39–44] and between individuals within the same species, with the intraspecific differences found among geographic locales [2,11,12,45–52], between sexes [46,47,53] and between juveniles and adults [9,46,47,54,55]. Venom variation has also been reported between venom glands of a single individual [56]. Some authors have argued that venom diversity is the product of neutral evolutionary processes and not subject to natural selection [57,58], whereas others have argued that strong natural selection has driven adaptation to particular prey species [12,30,31,40,46,47,59–63].

Venom in reptiles originated from a single early recruitment event approximately 180 million years ago (mya) during the early Jurassic period and is a plesiotypic trait of the Toxicofera clade [10,12,18,20–23,30,31,40,64]. New World pit vipers are thought to have descended from a single ancestral Asian pit viper species that colonized the New World via the Bering land bridge [65,66], with rattlesnakes having a mid-Cenozoic origin in the Mexican highlands [67–69]. The venom arsenals of Crotaline snakes are characterized by a great diversity of venom-components; generalized venom "types" have been proposed, depending upon metalloprotease activity and toxicity [70]. Type I venoms possess high levels of metalloprotease activity and lower toxicity (>1.0 μg/g mouse body weight), whereas type II venoms have low metalloprotease activity and higher toxicity (<1.0 μg/g mouse body weight). The presence of these two venom types in a diversity of well-defined species clades suggests that it is not dependent upon phylogeny [49,52,70–72].

Crotalus oreganus helleri is a medium-sized rattlesnake inhabiting Baja California northward through southern California, and the Pacific islands of Santa Catalina (Los Angeles County, California) and Coronado Del Sur (Tijuana, Mexico) [67]. Pronounced tectonic activity in the region has produced considerable variation in available habitat [73]. The species utilizes habitat ranging from sea level to >3000 m and prey encountered are highly varied. Significant regional variation in venom composition exists [51,74], with both type I and type II venoms identified in local populations [49]; however this dichotomy of venom types fails to characterize the full extent of venom variability in the species. *C. o. helleri* is the most medically relevant species of the region and is responsible for the majority of severe envenomations in southern California [29,75]. Therefore, determining intraspecific variation of *C. o. helleri* venom components and the factors influencing their molecular evolution can yield important implications for clinical treatment of envenomation. Venom variation also offers substantial potential for bioprospecting and pharmaceutical discovery [8,18–23,30,40,76]. These variations have been the subject of many popular press reports that grossly misattribute them to unparalleled recent diversification of the venom [77] and thus display a fundamental lack of understanding on how venom evolves.

In this study, we investigated the diversity of toxins present in *C. o. helleri*, across its geographic range, using a combined proteomics–transcriptomics approach to investigate the relative molecular evolution and diversification within a given toxin type, and the relative expression levels of particular toxin types.

2. Materials and methods

2.1. Sampling

We sampled four southern California populations of *C. o. helleri* from areas with pronounced geological, elevational, and floristic differences. Human envenomations from snakes in these

different regions have exhibited distinct symptoms ranging from hemorrhage to muscle fasciculations to paralysis. The four populations chosen (Fig. 1) were: (1) Catalina Island, which is dominated by coastal sage scrub, interspersed with chaparral and oak woodland, has never been connected to the mainland [73] and has supported an isolated population since at least the Pleistocene; (2) Idyllwild in the San Jacinto Mountains has high altitude pine and cedar montane forests (elevation ~1600 m); (3) Loma Linda consists of low rolling hills covered with grasses and, on north facing slopes, *Salvia mellifera* and other shrubs; and (4) Phelan comprises a transition zone between High Desert (Mohave) and coastal mountain scrub. We sampled one snake from each region for transcriptome sequencing. We used the same snake for proteome analysis of the Phelan and Loma Linda populations, and a separate individual of same sex and size from the exact same locality for the other two locations in addition to two more specimens for each location other than Loma Linda, for which only one more specimen was obtained due to the rarity of *C. o. helleri* in this location. We used only adult specimens for venom analysis due to potential ontogenetic shifts in venom composition [9,70].

2.2. Transcriptome sequencing, phylogenetics, selection analyses, and structural analyses

2.2.1. Transcriptome sequencing

Total RNA was extracted from venom glands using the standard TRIzol Plus method (Invitrogen). Extracts were enriched for mRNA using standard RNeasy mRNA mini kit (Qiagen) protocol. mRNA was reverse transcribed, fragmented and ligated to a unique 10-base multiplex identifier (MID) tag prepared using standard protocols and applied to one PicoTitrePlate (PTP) for simultaneous amplification and sequencing on a Roche 454 GS FLX + Titanium platform (Australian Genome Research Facility). An average of 50,000 sequences were read for each library. Automated grouping and analysis of sample-specific MID reads informatically separated sequences from the other transcriptomes on the plates, which were then post-processed to remove low quality sequences before de novo assembly into contiguous sequences (contigs) using v 3.4.0.1 of the MIRA software program. Assembly details for the transcriptomes are shown in Supplementary Table 1. All raw reads have been deposited in the NCBI Sequence Read Archive (http://www.ncbi.nlm.nih.gov/sra/) with the accession numbers of: SRR871501 *C. o. helleri* (Catalina Island), SRR871502 *C. o. helleri* (Idyllwild), SRR871503 *C. o. helleri* (Loma Linda), and SRR871504 *C. o. helleri* (Phelan). Assembled contigs were processed using CLC Main Work Bench (CLC-Bio) and Blast2GO bioinformatic suite to provide Gene Ontology, BLAST and domain/Interpro annotation. The above analyses assisted in the rationalization of the large numbers of assembled contigs into phylogenetic 'groups' for detailed phylogenetic analyses outlined below.

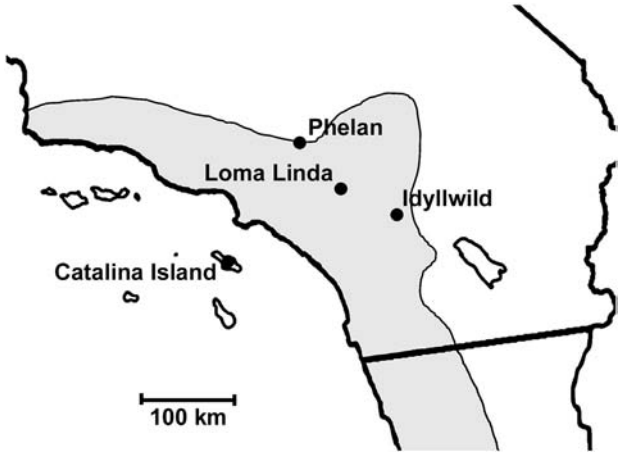

Fig. 1 – *C. o. helleri* populations investigated.

2.2.2. Selection analyses

Translated nucleotide sequences were aligned using MUSCLE 3.8 [78] and the alignments were manually inspected to rectify errors. All nucleotide sequences and multiple sequence alignments used for selection analyses are available as Supplementary file 2 and Supplementary Figs. 1–4, respectively. In order to reconstruct gene phylogenies for selection assessments, maximum-likelihood method implemented in PhyML [79] was employed on the nucleotide datasets and node support was evaluated with 1000 bootstrapping replicates. All the maximum-likelihood trees are provided as Supplementary Figs. 5–7, with the results of branch-site REL test mapped onto them. In order to detect the nature of selection and its influence on various venom-encoding genes of *C. o. helleri*, we utilized maximum-likelihood models implemented in Codeml of the PAML [80]. We employed site-specific models that estimate positive selection statistically as a non-synonymous-to-synonymous nucleotide-substitution rate ratio (ω) significantly greater than 1. For technical details regarding models/methods see [20,81]. FUBAR [82] implemented in HyPhy [83] was employed to provide additional support to the aforementioned analyses and to detect sites evolving under the influence of pervasive diversifying and purifying selection pressures. Mixed Effects Model Evolution (MEME) [82] was also employed to efficiently detect episodically diversifying sites. To clearly depict the proportion of sites under different regimes of selection, an evolutionary fingerprint analysis was carried out using the evolutionary selection distance (ESD) algorithm implemented in Datamonkey [84]. We further utilized the branch-site Random Effects Likelihood (REL) test [85] to identify lineages evolving under the influence of episodic diversifying selection pressures.

2.2.3. Structural analyses

To depict the natural selection pressures influencing the evolution of various *C. o. helleri* venom-components (only those with sufficient numbers of full-length sequences were analyzed in this regard: β-defensin, kallikrein and lectin), we mapped the sites under positive selection on the homology models created using Phyre 2 web server [86]. PyMOL 1.3 [87] was used to visualize and generate the images of homology models. ConSurf web server [88] was used for mapping the evolutionary selection pressures on the three-dimensional homology models.

Homology models of the presynaptic PLA_2 complex from *C. o. helleri* (Coh) (GenBank: GAKR01000015 [acid subunit] and GenBank: GAKR01000016 [basic subunit]) and the homologue from *Crotalus scutulatus scutulatus* (Css) (UniProt: P18998 [acid subunit] and UniProt: P62023 [basic subunit]) were built using the crystal structure of crotoxin from *Crotalus durissus terrificus* (Cdt)

(PDB: 3R0L; UniProt: P08878 [acid subunit]; UniProt: P0CG56 [basic subunit]) [89] as a template. Template to sequence alignments were generated using SPDBV [90,91] and exported as FASTA-formatted text. The 3R0L coordinates together with the alignment file were used for comparative modeling using MODELLER [92]. Images of these homology models were obtained using VMD [93] and Tachyon ray tracing. Charged surfaces were obtained by running the Adaptive Poisson–Boltzmann Solver APBS plug-in [94] to VMD. Representation in VMD was set to "orthographic", depth cueing was set to "off", and render mode was set to "GLSL".

2.3. Proteomics

2.3.1. HPLC

Lyophilized crude venom was diluted to a concentration of 3 mg/mL in Buffer A (0.065% TFA, 2% acetonitrile in Nanopure water) and centrifuged at 15,000 *g* for 10 min. The supernatant (100 μL) was fractionated on an ÄKTAmicro high-pressure liquid chromatography (HPLC) system (GE Healthcare Life Sciences, Piscataway, NJ, USA) fitted with two reversed-phase (RP) columns (SOURCE 5RPC ST polystyrene/divinyl benzene, 4.6 × 150 mm; GE Healthcare) run in series at a flow rate of 0.5 mL/min, using a linear gradient of 0–100% Buffer B (0.05% TFA, 80% acetonitrile in Nanopure water) over 40 column volumes. Protein elution was monitored at 214 nm using Unicorn 5.0 (GE Healthcare Life Sciences) software, and fractions were collected manually.

2.3.2. LC–MS

Each fraction was subjected to reduction and alkylation prior to enzymatic digestion using dithiothreitol and iodoacetamide, respectively, following the protocol outlined by Matsudaira [95]. Proteins were then digested with proteomics-grade porcine pancreatic trypsin (Sigma-Aldrich, St. Louis, MO, USA). We desalted samples using C_{18} ZipTips (EMD Millipore, Billerica, MA, USA) according to the manufacturer's protocol. The desalted tryptic peptides were resuspended in mobile phase A (2% acetonitrile, 0.1% formic acid in water). Liquid chromatography was conducted on a ThermoFinnigan LCQ Deca XP spectrometer (ThermoFinnigan, Waltham, MA, USA) equipped with a PicoView 500 nanospray apparatus using Xcalibur software (ver. 1.3; ThermoFinnigan, Waltham, MA, USA) for instrument control and data acquisition. Separation was performed on a 10-cm × 75-μm-i.d. C18 BioBasic bead column (New Objective, Woburn, MA, USA) by injecting 20-μL samples. Mobile phase B consisted of 98% acetonitrile, 2% water, and 0.1% formic acid. The gradient program was: 0% B at 0.18 mL/min for 7.5 min; 0% B at 0.35 mL/min for 0.5 min; linear gradient to 20% B at 15 min at 0.35 mL/min; linear gradient to 75% B at 55 min at 0.3 mL/min (flow rate constant for remainder of the program); linear gradient to 90% B at 60 min; hold at 90% B until 85 min; linear gradient to 0% B at 90 min; hold at 0% B until 120 min. Spectra were acquired in positive ion mode with a scan range of 300–1500 m/z. We converted MS/MS data into peak list files using ExtractMSn implemented in BioWorks (version 3.1; ThermoFinnigan) with the following parameters: peptide molecular weight range of 300–3500, threshold of 100,000, precursor mass tolerance of 1.4, and minimum ion count of 35. We conducted MS/MS database searches using Mascot (licensed, version 2.2, Matrix Science, Boston, MA, USA) against the National Center for Biotechnology Information non-redundant (NCBInr) database in the taxon Metazoa with a parent tolerance of 1.20 Da, fragment tolerance of 0.60 Da, and two missed trypsin cleavages allowed. We

Table 1 – C. o. *helleri* intraspecific proteomic and transcriptomic toxin presence.

Toxin molecular scaffold type	Catalina Island		Idyllwild		Loma Linda		Phelan	
	P	T	P	T	P	T	P	T
β-defensin	Large amounts, medium complexity	✓	Large amounts, medium complexity	✓	Large amounts, medium complexity	✓	Large amounts, medium complexity	✓
CNP-BPP	Medium amounts, low complexity	✓	Low amounts, low complexity	✓	Large amounts, low complexity	✓	Large amounts, low complexity	✓
CRiSP	Large amounts, medium complexity	✓	✖	✓	Medium amounts, low complexity	✓	Medium amounts, medium complexity	✖
Hyaluronidase	✖	✓	✖	✓	✖	✓	✖	✓
Kallikrein	Medium amounts, low complexity	✓	Medium amounts, high complexity	✓	Large amounts, high complexity		Large amounts, high complexity	✓
Kunitz	✖	✓	✖	✓	✖	✓	✖	✓
L-Amino acid oxidase	Medium amounts, low complexity	✓	Medium amounts, low complexity	✓	Medium amounts, low complexity	✓	Medium amounts, low complexity	✓
Lectin	Large amounts, medium complexity	✓	✖	✖	✖	✓	Low amounts, low complexity	✓
Nerve growth factor	Low amounts, low complexity	✓	✖	✓	Low amounts, low complexity	✓	✖	✖
Phospholipase A_2	Medium amounts, medium complexity	✓	Large amounts, high complexity	✓	Low amounts, low complexity	✓	Low amounts, low complexity	✓
Snake venom metalloprotease	Large amounts, medium complexity	✓	Not detected	✓	Medium amounts, high complexity	✓	Large amounts, high complexity	✓
Vascular endothelial growth factor	✖	✓	✖	✓	Low amounts, low complexity	✓	Low amounts, low complexity	✓
Vespryn	✖	✓	✖	✓	✖	✓	✖	✓

P = proteome.
T = transcriptome.

specified carbamidomethylation of cysteine and oxidation of methionine in Mascot as fixed and variable modifications, respectively.

2.3.3. *MALDI ToF MS and MALDI ToF/ToF MS/MS*

RP-HPLC fractions were submitted to the Institute for Integrated Research in Materials, Environments and Society at California State University, Long Beach, to determine whole protein molecular masses and protein identification/similarity. For MALDI ToF/ToF MS/MS analysis, tryptic peptides were mixed with α-cyano-4-hydroxy cinnamic acid (CHCA) matrix and directly spotted onto MALDI plates. MS spectra were collected using 1000 laser shots/spectrum, and MS/MS spectra from 3000 shots/spectrum. Peptides with signal-to-noise ratio above 15 in MS mode were selected for MS/MS analysis, with a maximum of 15 MS/MS spectra allowed per spot. Internal calibration was achieved using ToF/ToF Calibration Mixture (AB SCIEX). We searched MS/MS data against the NCBInr database within Metazoa using GPS Explorer, running Mascot (version 2.1) search engine with a peptide tolerance of 300 ppm, MS/MS tolerance of 0.8 Da, and one missed cleavage allowed. We specified carbamidomethylation of cysteine as a fixed modification, and the following as variable modifications: carbamyl, Gln/pyro-Glu (N-term Q), and Glu/pyro-Glu (N-term E). Mass spectrometry data for the peaks in Supplementary File 1 is presented in Supplementary Spreadsheet 1.

2.3.4. *Statistical analyses*

To confirm that population differences existed among the 11 snakes with the quantitative RP-HPLC data presented in Supplementary Spreadsheet 2, we subjected the percent protein present in each of the 11 toxin families (area under the peaks) to a 4 × 11 (population × toxin family) analysis of variance (ANOVA [96]), treating population as a between-subjects factor and toxin family as a within-subjects factor. We rank-transformed the data to avoid analysis of percentage data that summed to 100 for

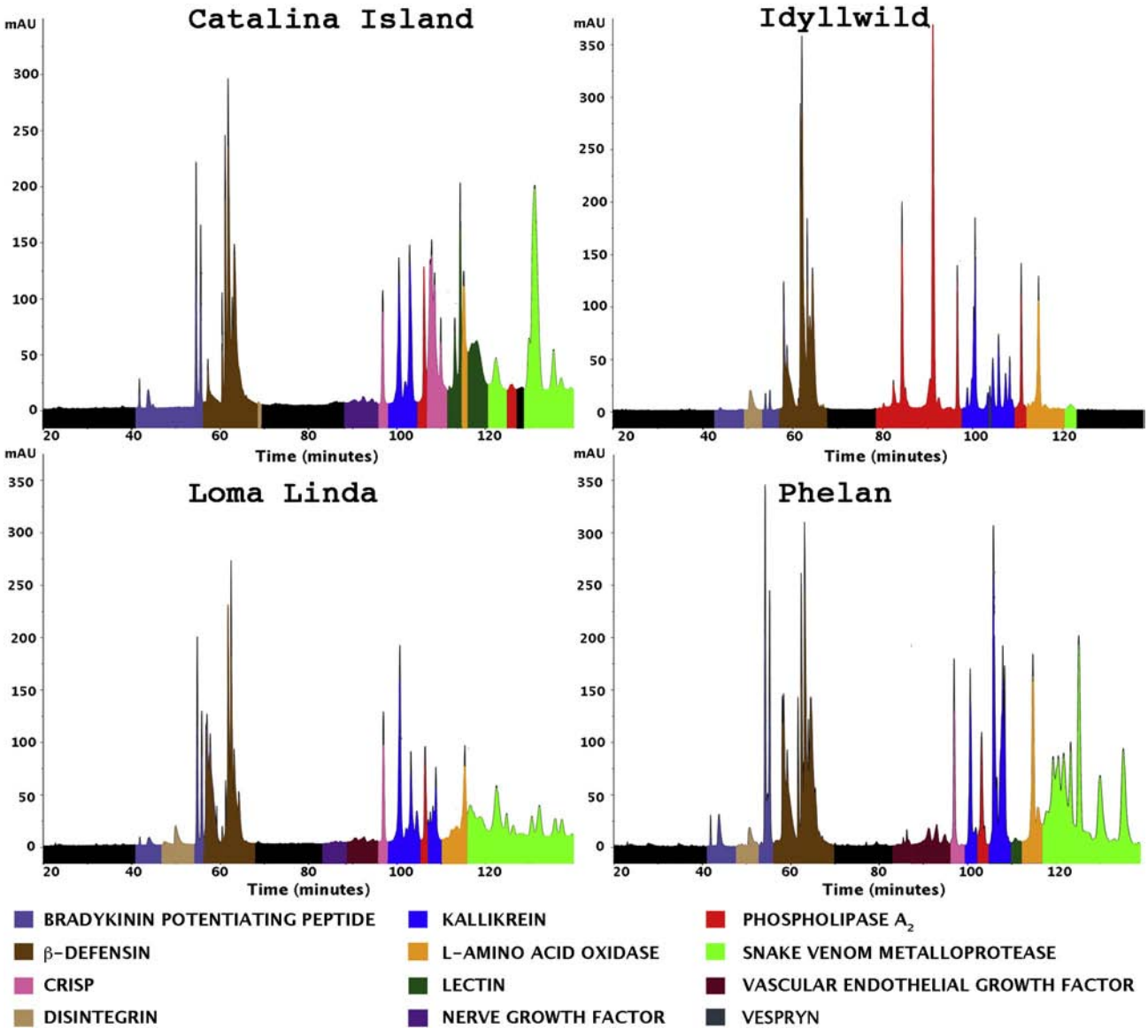

Fig. 2 – LC–MS/MS annotated RP-HPLC chromatograms from the four different *C. o. helleri* populations examined in this study.

each individual. Although our samples were small and data were somewhat non-normal and heteroscedastic, general linear models generally handle data well that fail to meet parametric assumptions and the results were extremely robust. We also ran a non-parametric Kruskal–Wallis ANOVA for each toxin family to compare the populations, which allowed us to confirm the results from the parametric ANOVA; this latter test requires no assumptions about data distribution [96]. We computed effect

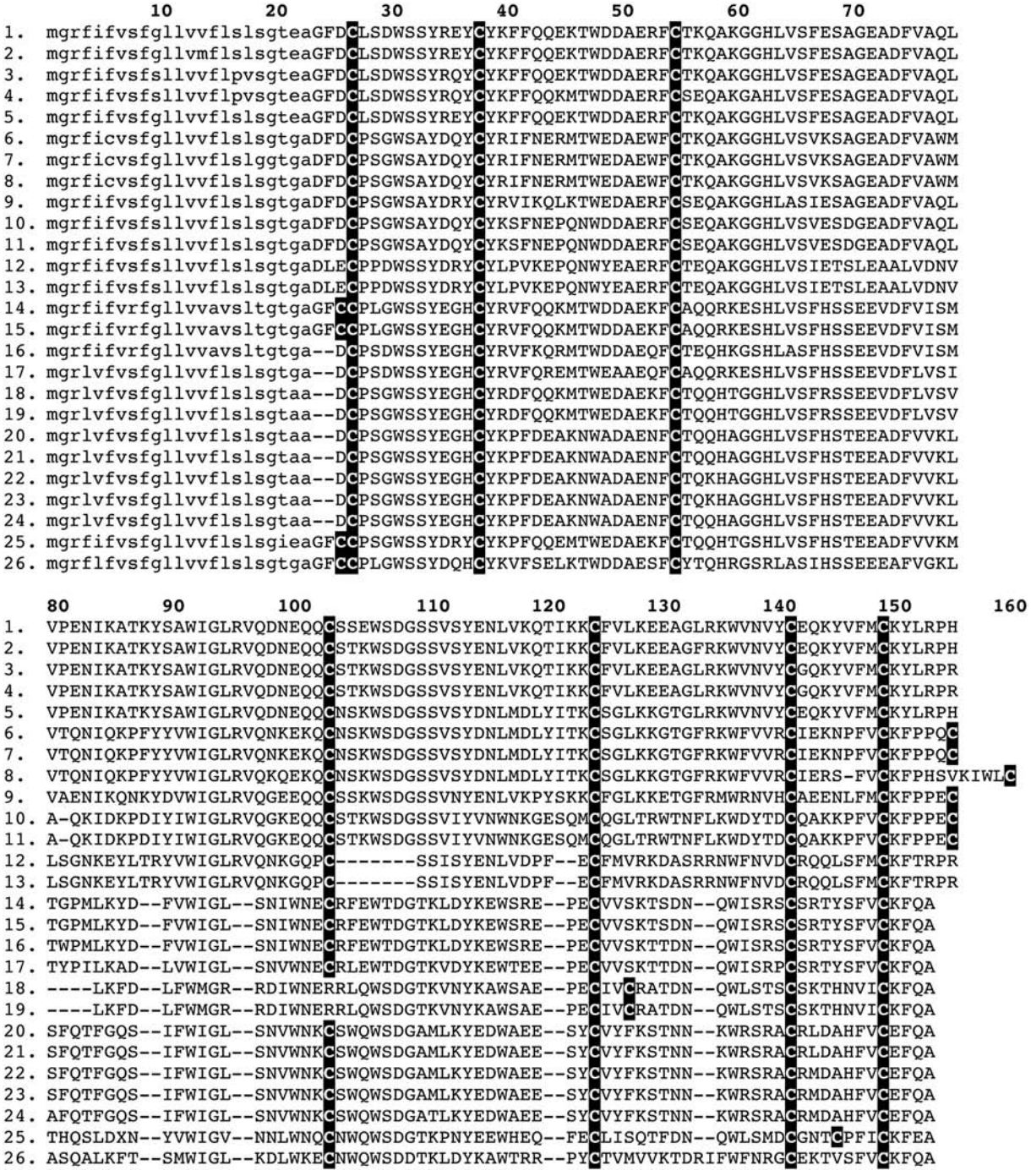

Fig. 3 – Sequence alignment of lectins from *C. o. helleri*: α) 1. GAKQ01000018 CohCI-5, 2. GALC01000015 CohLL-3, 3. GAKQ01000016 CohCI-3, 4. GAKS01000016 CohPH-3, 5. GAKQ01000015 CohCI-2, 6. GAKQ01000014 CohCI-1, 7. GALC01000013 CohLL-1, 8. GAKS01000014 CohPH-1, 9. GALC01000014 CohLL-2, 10. GAKQ01000017 CohCI-4, 11. GAKS01000017 CohPH-4, 12. GALC01000017 CohLL-5, 13. GALC01000016 CohLL-4; and β) 14. GALC01000020 CohLL-3, 15. GALC01000018 CohLL-1, 16. GALC01000022 CohLL-5, 17. GAKS01000021 CohPH-4, 18. GAKS01000022 CohPH-5, 19. GALC01000021 CohLL-4, 20. GAKQ01000022 CohCI-4, 21. GAKQ01000021 CohCI-3, 22. GAKQ01000020 CohCI-2, 23. GAKQ01000019 CohCI-1, 24. GAKS01000019 CohPH-1, 25. GAKS01000020 CohPH-3, 26. GAKS01000023 CohPH-6. CI = Catalina Island, LL = Loma Linda, PH = Phelan. Signal peptide is shown in lowercase, cysteines are highlighted in black.

sizes (approximate variance explained) as adjusted partial eta-squared (η^2) for the parametric ANOVA and as η^2 (computed as χ^2 / [total N – 1]) for the Kruskal–Wallis ANOVAs [96,97]. Eta-squared values ≥ 0.14 are generally deemed large [98]. We conducted these analyses using SPSS 13.0 for Windows, with alpha = 0.05. Following Nakagawa [99], we did not apply Bonferroni adjustments to multiple tests.

3. Results and discussion

Random sequencing recovered sequences for 13 different venom protein encoding gene families (Table 1), with all but Kunitz and Hyaluronidase recovered by both proteomics and transcriptomics. The inability of our combined approach to detect these two venom-components in both result sets may be due to a number of factors, such as, i) differential transcription/translation: not all toxins being replenished at equal stoichiometric rates or simultaneously; ii) technical limitation: the relative separation ability of the HPLC column utilized; iii) co-elution of toxins: one toxin type dominating another and thus obscuring the signal of a toxin present in significantly lower amounts; iv) transcriptomics: the non-exhaustive random sampling procedure utilized which would statistically be likely to recover the most abundant toxin types, with lower-level expressed toxins not recovered; and/or v) microRNA silencing: whereby toxin coding regions undergo transcription but not translation [100]. Lectin toxins, however, were conspicuously absent in both the proteomics and transcriptomics of the Idyllwild population. Sequences analyzed in this study have the GenBank accession numbers of: *C. o. helleri* (Catalina Island) GAKQ01000001–GAKQ01000026; *C. o. helleri* (Idyllwild) GAKR01000001–GAKR01000018; *C. o. helleri* (Loma Linda) GALC01000001–GALC01000026; and *C. o. helleri* (Phelan) GAKS01000001–GAKS01000031. It must be noted that in accordance with the new GenBank deposition rules to exclude fragments of less than 200 base pairs, only the full length sequences were deposited. Thus 27 β-defensins were not deposited, even though their processed and secreted toxin regions were sequenced (only regions of the signal peptide were incomplete). Thus, while these sequences could not be deposited into GenBank, they were utilized in the analyses and are included in the Supplementary material.

Our proteomics analyses revealed significant differences in the venoms of the four populations (Fig. 2), with venom RP-HPLC profiles within a population largely congruent among individuals (Supplementary Fig. 8; note: only two Loma Linda specimens were able to be analyzed due to the rarity of *C. o. helleri* in this locality). The parametric ANOVA yielded a highly significant interaction between population and toxin family ($F_{9.8,22.9} = 13.15$, $P < 0.001$, adjusted partial $\eta^2 = 0.31$; Greenhouse–Geisser adjustment of degrees-of-freedom applied), indicating that the distribution of toxins among the toxin families differed significantly among the populations. The Kruskal–Wallis ANOVAs confirmed that toxin quantity varied significantly among populations for some (nerve growth factor, cysteine-rich secretory protein [CRiSP], lectin; all $P = 0.21$–0.35, $\eta^2 = 0.86$–0.97) but not all toxin families. Five additional toxins (BPP, β-defensin, kallikrein, PLA_2, SVMP) approached significance ($P < 0.10$) with exceptional effect sizes ($\eta^2 > 0.63$). Thus, the ANOVAs confirmed population differences despite the small sample sizes.

Some toxin types were notable for being either highly conserved in their coding sequences (β-defensin, natriuretic), whereas others were extremely variable (kallikrein, lectin, PLA_2, SVMP). While the β-defensins and bradykinin potentiating peptides (BPPs) were of low complexity, our proteomics analyses of the relative expression levels revealed that they are expressed

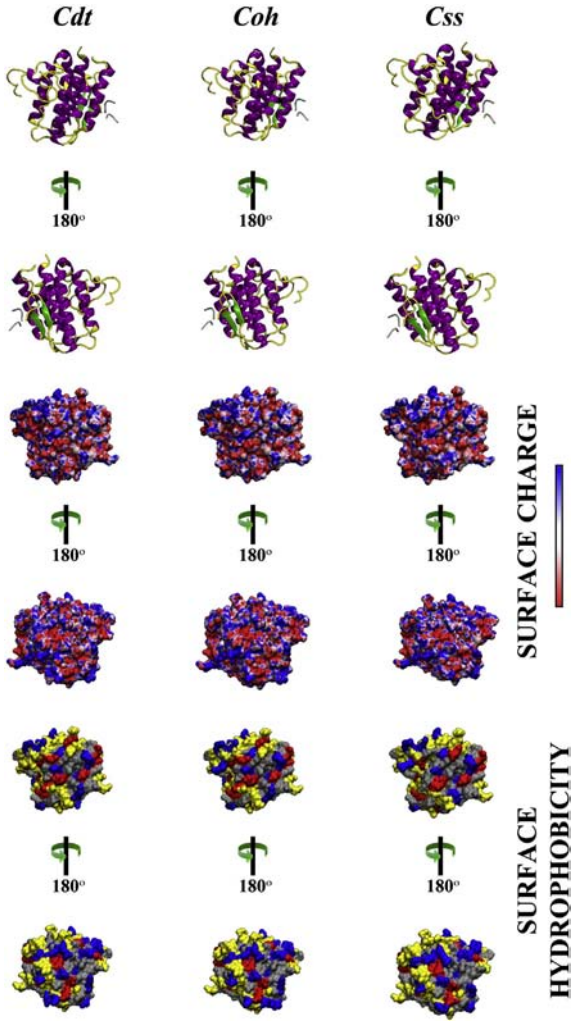

Fig. 4 – Comparative ribbon, surface charge and surface hydrophobicity of the hetrodimeric presynaptic neurotoxic phospholipase A_2 complex from the venoms of *Crotalus durissus terrificus* (Cdt) (PDB: 3R0L; UniProt: P08878 [acidic subunit]; UniProt: P0CG56 [basic subunit]), *C. o. helleri* (Coh) (GenBank: GAKR01000015 [acidic subunit] and GenBank: GAKR01000016 [basic subunit]) and *Crotalus scutulatus scutulatus* (Css) (UniProt: P18998 [acidic subunit] and UniProt: P62023 [basic subunit]). Cartoon images show helices in purple, sheets in green and other structural regions in yellow. Surface charge potentials were mapped on surfaces allowing for color scale data range values of –10.00 to +10.00 using the RWB coloring scheme. Surface residue hydrophicity mapping of residue-type surfaces depicts acidic residues in red, basic residues in blue, polar residues in yellow, and nonpolar residues in silver.

in very high amounts in all populations, with β-defensin in particular invariantly expressed in large quantities (Fig. 2). The multi-product natriuretic/BPP precursor was invariant within and between populations in both the plesiotypic natriuretic peptide domain and the apotypic (derived) BPP domains located within the propeptide region. In contrast, the lectin sequences were highly variable, including the apotyposis of novel cysteines which may facilitate novel structural folding or unique subunit formation with lectins or other toxin types (Fig. 3). Consistent with the proteomic results of this study and a previously published study of San Jacinto Mountain specimens [49] as well as observed notable clinical effects, only the Idyllwild population contained both the acidic and basic subunits of the neurotoxic PLA_2 complex type, with both chains virtually identical to the well-characterized potent presynaptic neurotoxins from *C. d. terrificus* and *C. s. scutulatus* (Fig. 4). It was also notable that the Idyllwild population secreted the lowest amount of SVMPs (Fig. 2), with only a single isoform obtained in the transcriptome and only detectable in trace levels in the proteome. In contrast, the other populations secreted SVMPs in large amounts, with the Phelan having the greatest complexity while the Catalina Island population had less complexity but a much higher relative expression level. This is consistent with the pattern observed for *C. s. scutulatus*, that there is an inverse relationship between the relative amount of neurotoxic PLA_2 and hemorrhagic SVMP [37,101,102]. Thus, it is quite evident how a biochemical arsenal with such variability in neurotoxic, hemotoxic and myotoxic venom-components can complicate clinical treatment of bite victims, not only through the production of highly variable clinical effects, but also as a consequence the reciprocal variability in the efficacy of antivenom binding. It should be noted that the venom proteomics of

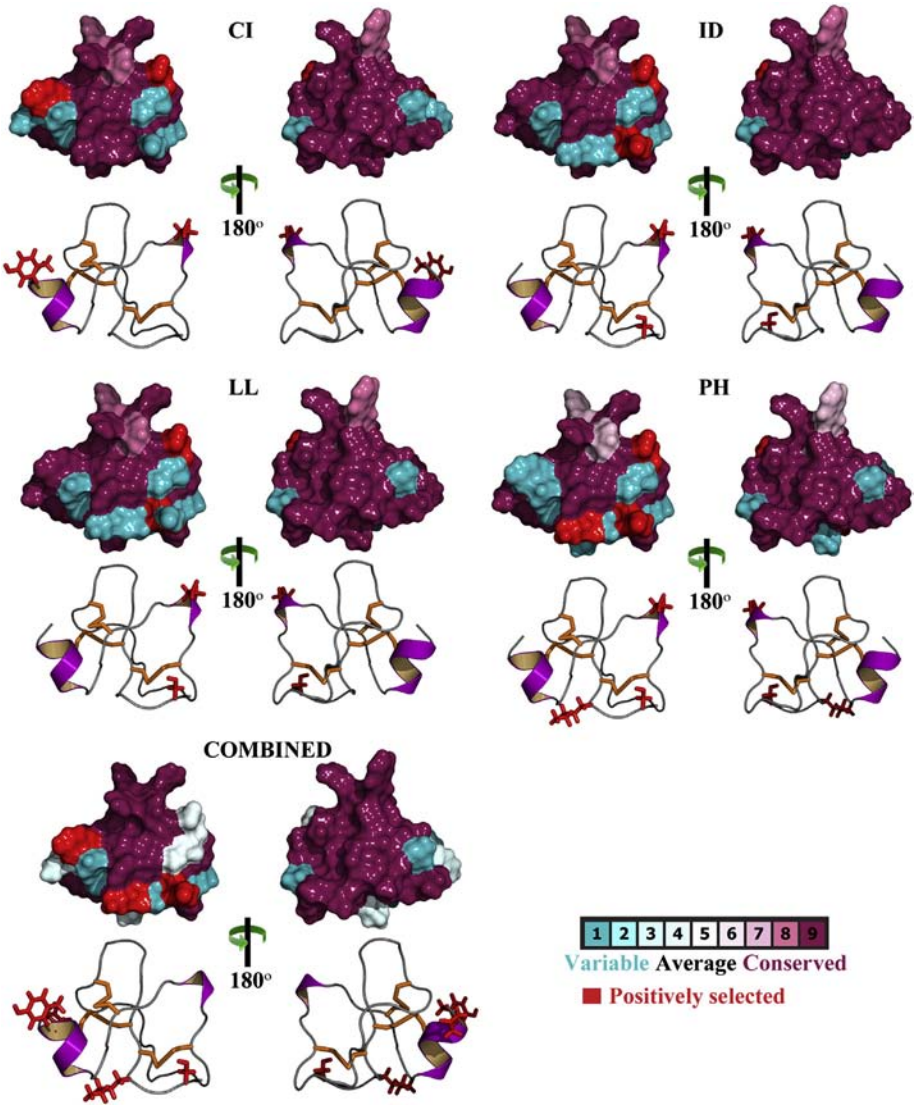

Fig. 5 – Molecular evolution of *C. o. helleri* β-defensins. Three-dimensional homology models (built using the PDB template 1Z99) of β-defensins with evolutionary conservation of amino acids mapped onto them, depicting the locations of positively selected sites (in red) detected by site-model 8 (PP ≥ 0.95, BEB). Schematic representation of the models, which not only depicts the locations of positively selected sites (red sticks) but also highlights disulfide bonds (orange sticks), α helices (purple) and β sheets (green), are also presented.

multiple animals (n = 3; except Loma Linda population, where these animals are extremely rare) from the same region were fairly similar. Hence, it can be safely assumed that the venom-gland transcriptomics of randomly chosen animals represents the overall venomics (genetic makeup of the venom gland) of the representative population.

Understanding the nature and strength of natural selection pressures, which sculpt genetic diversity, is the central theme of molecular evolutionary studies. Since non-synonymous mutations are more likely to influence the structure and function of a protein and hence in turn influence the fitness of the organism, evaluating the rate of accumulation of non-synonymous mutations (dN) in genes, relative to synonymous mutations (dS), as a ratio known as ω (or dN/dS ratio), is essential. We assessed the role of evolutionary selection pressures in shaping various venom proteins in different populations of *C. o. helleri* using various state-of-art selection assessment methodologies. We detected a significant influence of positive Darwinian selection on the evolution of most venom protein encoding genes in these snakes (Figs. 5–7; Tables 2–4; Supplementary Tables 2–5; Supplementary Figs. 1–7 and 9–11).

Site-specific selection assessments indicated that β-defensins, which were expressed in relatively large amounts by all *C. o. helleri* populations examined, followed a regime of weak positive selection: Catalina Island: ω = 1.33 and 3 positively selected (PS); Idyllwild: ω = 2.07 and 3 PS; Loma Linda: ω = 1.14 and 2 PS; Phelan: ω = 1.31 and 5 PS; All: ω = 1.18 and 11 PS (Fig. 5; Table 2). However, the mapping of mutations onto sequence alignments indicated that most hypermutable sites detected by site-specific methods in β-defensins were concentrated in the non-secreted regions of the toxin that are not likely to contribute in the envenoming process. It was also evident

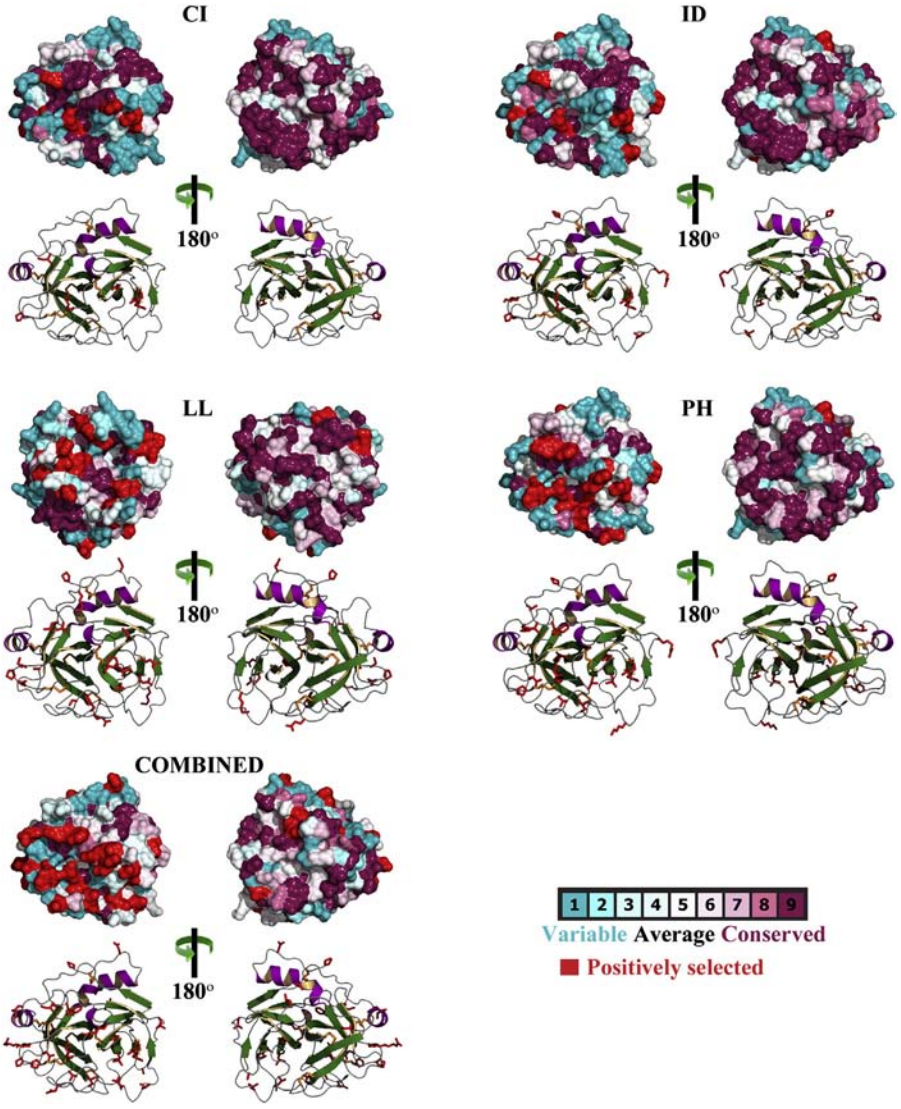

Fig. 6 – Molecular evolution of *C. o. helleri* kallikreins. Three-dimensional homology models (Loma Linda population modeled using the PDB template 1OP0; all others using 2AIQ) of kallikreins with evolutionary conservation of amino acids mapped onto them, depicting the locations of positively selected sites (in red) detected by site-model 8 (PP ≥ 0.95, BEB) are presented. Schematic representation of the models, which not only depicts the locations of positively selected sites (red sticks) but also highlights disulfide bonds (orange sticks), α helices (purple) and β sheets (green), are also presented.

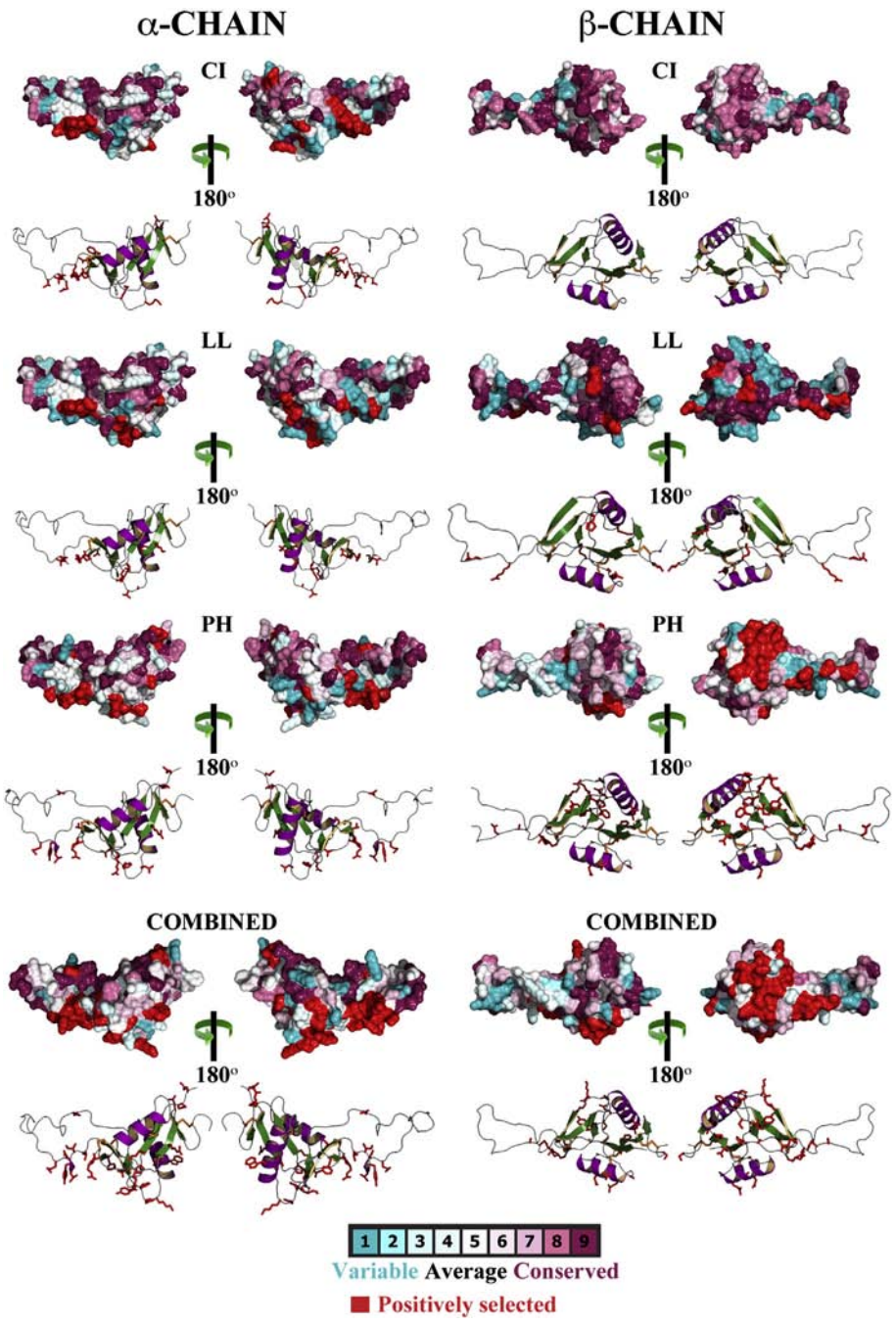

Fig. 7 – Molecular evolution of *C. o. helleri* lectin α- and β-chains. Three-dimensional homology models (α-chain lectins: Catalina Island population and the 'combined set' modeled using PDB template 1C3A; others using 1UMR; β-chain lectins: Loma Linda population modeled using the template 1V4L; all others using 1J34) of lectin α- and β-chains with evolutionary conservation of amino acids mapped onto them, depicting the locations of positively selected sites (in red) detected by site-model 8 (PP ≥ 0.95, BEB). Schematic representation of the models, which not only depicts the locations of positively selected sites (red sticks) but also highlights disulfide bonds (orange sticks), α helices (purple) and β sheets (green), are also presented.

that the entire stretch of nucleotides encoding the secreted region of β-defensins evolved under the extreme influence of negative selection, with 76% of residues being extremely well conserved (percent identity ≥ 90%; Supplementary Fig. 1). This was also supported by the results of MEME, an extremely accurate method of detecting episodic bursts of adaptation, which detected fewer episodically diversifying sites in β-defensins (Table 2). Mapping of variable sites on the structure of the β-defensin 'crotamine' from *C. d. terrificus* (PDB code: 1Z99 [103]), which is homologous and thus structurally very similar

Table 2 – C. o. *helleri* intraspecific venom dynamics: β-defensins.

Population	FUBAR [a]	MEME sites [b]	BSR [c]	PAML [d]	
				M8	M2a
CI	ω > 1 [e]: 0 ω < 1 [f]: 1	0	1	3 (2 + 1) 1.33	3 (2 + 1) 1.33
ID	ω > 1 [e]: 1 ω < 1 [f]: 0	0	2	3 (2 + 1) 2.07	3 (2 + 1) 2.07
LL	ω > 1 [e]: 0 ω < 1 [f]: 0	1	1	2 (0 + 2) 1.14	0 1.14
PH	ω > 1 [e]: 1 ω < 1 [f]: 1	0	4	5 (1 + 4) 1.31	2 (1 + 1) 1.31
Combined	ω > 1 [e]: 0 ω < 1 [f]: 0	4	6	11 (5 + 6) 1.18	6 (3 + 3) 1.16

ω: mean dN/dS.
Populations: CI = Catalina Island; ID = Idyllwild; LL = Loma Linda; PH = Phelan.
[a] Fast Unconstrained Bayesian AppRoximation.
[b] Sites detected as experiencing episodic diversifying selection (0.05 significance) by the Mixed Effects Model Evolution (MEME).
[c] Number of branches detected by the branch-site REL (random effects likelihood) test as episodically diversifying.
[d] Positively selected sites detected by the Bayes Empirical Bayes approach implemented in M8 and M2a. Sites detected at 0.99 and 0.95 significance are indicated in the parenthesis.
[e] Number of sites under pervasive diversifying selection at the posterior probability ≥ 0.9 (FUBAR).
[f] Number of sites under pervasive purifying selection at the posterior probability ≥ 0.9 (FUBAR).

Table 3 – C. o. *helleri* intraspecific venom dynamics: Kallikrein.

Population	FUBAR [a]	MEME sites [b]	BSR [c]	PAML [d]	
				M8	M2a
CI	ω > 1 [e]: 8 ω < 1 [f]: 5	6	4	7 (6 + 1) 1.35	7 (4 + 3) 1.31
ID	ω > 1 [e]: 20 ω < 1 [f]: 4	6	6	11 (2 + 9) 1.63	11 (2 + 9) 1.63
LL	ω > 1 [e]: 23 ω < 1 [f]: 8	9	9	24 (8 + 16) 1.60	15 (7 + 8) 1.57
PH	ω > 1 [e]: 22 ω < 1 [f]: 7	15	5	24 (10 + 14) 1.38	15 (7 + 8) 1.41
Combined	ω > 1 [e]: 27 ω < 1 [f]: 14	45	12	36 (18 + 18) 1.36	25 (13 + 11) 1.38

ω: mean dN/dS.
Populations: CI = Catalina Island; ID = Idyllwild; LL = Loma Linda; PH = Phelan.
[a] Fast Unconstrained Bayesian AppRoximation.
[b] Sites detected as experiencing episodic diversifying selection (0.05 significance) by the Mixed Effects Model Evolution (MEME).
[c] Number of branches detected by the branch-site REL (random effects likelihood) test as episodically diversifying.
[d] Positively selected sites detected by the Bayes Empirical Bayes approach implemented in M8 and M2a. Sites detected at 0.99 and 0.95 significance are indicated in the parenthesis.
[e] Number of sites under pervasive diversifying selection at the posterior probability ≥ 0.9 (FUBAR).
[f] Number of sites under pervasive purifying selection at the posterior probability ≥ 0.9 (FUBAR).

to β-defensin, revealed that the N-terminal positions 23 (Y in sequence 1; Supplementary Fig. 1) and 25 (R in sequence 1; Supplementary Fig. 1) as well as the C-terminal residues in position 61 (K in sequence 1; Supplementary Fig. 1), 62 (S in sequence 1; Supplementary Fig. 1), and 63 (G in sequence 1; Supplementary Fig. 1) are structurally more flexible (for the remaining positively selected amino acids 3D-structure coordinates were not resolved). This can be explained by the fact that these locations in the protein structure fall outside the disulfide bond-stabilized core. Although the highly conserved positions, such as 28 (K), 53 (R), 54 (W), and 55 (R; all referred to in sequence 1; Supplementary Fig. 1) were also solvent exposed, they were located inside the disulfide bridge-stabilized protein core and thus experienced heavy constraints of negative selection. However, the lack of variation in secreted regions of β-defensins may be indicative of their unique mode of action as peptides non-specifically target and destabilize the negatively charged microbial membranes using their cationic amino acid residues, resulting in membrane permeabilization [104]. Not-surprisingly, 29% of the residues in *C. o. helleri* β-defensins were cationic (K, R and H) and were extremely well conserved (percent identity ≥ 80%; Supplementary Fig. 1). Hence, it is expected that the evolutionary constraints favor the preservation of cationic residues required for toxicity. The branch-site REL (BSR) test, which significantly identifies lineages that follow the regime of episodic diversification, clearly highlighted the differences in strengths of evolutionary selection pressures acting upon β-defensins in *C. o. helleri* populations (Supplementary Fig. 5). In the Phelan population this test detected as many as four episodically diversifying branches in β-defensin gene lineage, while detecting only one branch each in Catalina Island and Loma Linda populations, and two branches in the Idyllwild population (Supplementary Fig. 5).

While the kallikreins found in each of the *C. o. helleri* populations examined were found to be rapidly evolving under the influence of positive selection [Catalina Island: ω = 1.35 and 7 PS; Idyllwild: ω = 1.63 and 11 PS; Loma Linda: ω = 1.60 and 24 PS; Phelan: ω = 1.38 and 24 PS; All: ω = 1.36 and 36 PS] (Fig. 6; Supplementary Fig. 2), the number of positively selected sites detected by M8's Bayes empirical Bayes (BEB) approach, varied from 7 to 24, highlighting the differential rate of evolution of kallikreins in various *C. o. helleri* populations (Table 3). The number of branches detected by the BSR test as episodically diversifying in kallikrein encoding genes varied from 4 to 10 in various populations (Supplementary Fig. 6), again highlighting the differential role of selection in shaping these venom protein encoding genes.

Lectin α-chain [Catalina Island: ω = 2.36 and 15 PS; Loma Linda: ω = 2.51 and 14 PS; Phelan: ω = 3.07 and 16 PS; All: ω = 2.23 and 27 PS] and lectin β-chain [Catalina Island: ω = 0.46 and 0 PS; Loma Linda: ω = 2.73 and 11 PS; Phelan: ω = 2.34 and 28 PS; All: ω = 2.29 and 29 PS] were found to evolve under the significant

Table 4 – C. o. *helleri* intraspecific venom dynamics: Lectins.

Population	FUBAR [a]	MEME sites [b]	BSR [c]	PAML [d]	
				M8	M2a
α chain					
CI	ω > 1 [e]: 12 ω < 1 [f]: 5	2	4	15 (8 + 7) 2.36	12 (5 + 7) 2.34
LL	ω > 1 [e]: 15 ω < 1 [f]: 2	1	3	14 (7 + 7) 2.51	12 (5 + 7) 2.51
PH	ω > 1 [e]: 15 ω < 1 [f]: 4	0	4	16 (8 + 8)	13 (7 + 6)
Combined	ω > 1 [e]: 26 ω < 1 [f]: 6	7	7	27 (14 + 13) 2.23	23 (14 + 9) 2.24
β chain					
CI	ω > 1 [e]: 0 ω < 1 [f]: 1	0	0	0 0.46	0 0.46
LL	ω > 1 [e]: 2 ω < 1 [f]: 0	0	1	11 (0 + 11) 2.73	2 (0 + 2) 2.73
PH	ω > 1 [e]: 16 ω < 1 [f]: 2	5	6	28 (12 + 16) 2.34	22 (9 + 13) 2.34
Combined	ω > 1 [e]: 22 ω < 1 [f]: 2	5	6	29 (16 + 13) 2.29	20 (11 + 9) 2.31

ω: mean dN/dS.
Populations: CI = Catalina Island; ID = Idyllwild; LL = Loma Linda; PH = Phelan.
[a] Fast Unconstrained Bayesian AppRoximation.
[b] Sites detected as experiencing episodic diversifying selection (0.05 significance) by the Mixed Effects Model Evolution (MEME).
[c] Number of branches detected by the branch-site REL (random effects likelihood) test as episodically diversifying.
[d] Positively selected sites detected by the Bayes Empirical Bayes approach implemented in M8 and M2a. Sites detected at 0.99 and 0.95 significance are indicated in the parenthesis.
[e] Number of sites under pervasive diversifying selection at the posterior probability ≥ 0.9 (FUBAR).
[f] Number of sites under pervasive purifying selection at the posterior probability ≥ 0.9 (FUBAR).

influence of positive selection (Table 4; Supplementary Fig. 3). However, β-chain of the Catalina Island population was remarkably revealed to have evolved under the influence of negative selection (ω = 0.46, 0 PS; Table 4; Supplementary Fig. 4). Other than at position 56, amino acid residues in all other positions were invariant (Supplementary Fig. 4). The rapid rate of molecular evolution observed in lectins is consistent with the great diversity of novel sequences recovered, including the apotyposis or the derivation of novel cysteine residues (Fig. 3). The rapid accumulation of hypermutable sites under the influence of positive selection in β-chain lectins from all *C. o. helleri* populations except those from Catalina Island, where the toxin-encoding gene has evolved under strong negative selection, is intriguing and warrants further experimental evaluations to understand the stark differences in the magnitude of selection pressures. While the BSR test detected a few lineages as episodically diversifying in the α-chain lectins of various populations, the results of this test in the β-chain lectins were particularly interesting (Supplementary Fig. 7). This test failed to detect any branch in the Catalina Island population, while detecting a single branch in Loma Linda population as episodically diversifying (Supplementary Fig. 7). In contrast, as many as 6 branches were detected as following the regime of episodic adaptation in β-chain lectins of the Phelan population (Supplementary Fig. 7). Similar to the results of all state-of-art selection assessment methods outlined above, the evolutionary fingerprints of venom-encoding genes in *C. o. helleri* clearly depicted the differential influence of natural selection on their evolution (Supplementary Figs. 9–11).

The structure and surface chemistry of the presynaptic PLA_2 complex from *C. o. helleri* is very well conserved when compared to the homologues from *C. d. terrificus* and *C. s. scutulatus* (Fig. 4). Both amino acid type distribution on the protein surface as well as studying surface charges and surface hydrophobicity of all three PLA_2 complexes revealed only minor differences. While the positive and negative charged patches in globo were located in the same positions, minimal differences were observed in the size and charge of these surface regions. Since the PLA_2s of *C. d. terrificus* and *C. s. scutulatus* are well-characterized to be potent neurotoxins (cf. [89,105]), we conclude that the described similarities of *C. o. helleri* PLA_2 to the former ones are responsible for neurotoxic effects of PLA_2s observed in the *C. o. helleri* population. The precise evolutionary regimes followed by genes encoding PLA_2 and SVMPs in these snakes remain to be elucidated.

Thus, it is evident that *C. o. helleri* venom-encoding genes have experienced differential evolutionary selection pressures. Differential rate of molecular evolution or expression occurred not only between toxin types within the venom of a particular population, but also for the same toxin type between populations. These results demonstrate that the different populations of *C. o. helleri* follow distinct evolutionary trajectories, with the differential venom profiles likely driven by variation in predatory ecology. This is a reflection of the complex evolutionary history of this species, which ranges from sea level to high mountain peaks and occupies a diverse range of habitats. These habitats possess differing lizard and mammal prey assemblages [106–108], and evidence from other snakes suggests that strong natural selection has driven venom adaptation to particular prey species [12,20,21,30,31,40,46,47,59,61–63,109]. Although climate might be expected to influence venom composition, our data suggest otherwise concerning the dichotomy of type I (proteolytic or "tenderizer") versus type II (more toxic) venoms [70]. It has been suggested that snakes at higher elevation with the greatest temperature fluctuations could be expected to possess a type I venom to facilitate digestion [70]. However, the population that faces the highest temperature fluctuations (Idyllwild) possesses a type II venom that lacks almost entirely the metalloproteases typical of type I venoms. These results also indicate significant differences in potential human envenomation profiles, consistent with the complex clinical picture previously observed, with some populations being hemorrhagic while others are neurotoxic. The exquisite diversity of venom-components highlighted in this study and the variation in intensity and the nature of natural selection shaping the molecular toxin scaffolds may not only result in distinct envenoming profiles but may also induce variable responses to antivenom. Hence, understanding the true molecular diversity of venom and the evolutionary forces that shape them not only

aids in the prediction of clinical effects but also reveals that these highly variable venoms are a rich source of novel toxins, some of which may have significant potential for use as lead compounds in drug design and development. Thus, the results of this study not only contribute to the body of knowledge regarding venom evolution but also have applied outcomes both from a clinical perspective and also from drug design. These results will also be useful in science communication to demonstrate that there is indeed significant variation in the venom of this medically important species, but that such evolution has not occurred recently but rather the venom diversity seen today is reflective of the long evolutionary history, not of recent changes as popularly misunderstood. Thus this species is a model for the broader penetration of lay-person understanding of venom diversity and the clinical and economic importance of such variation.

Acknowledgments

BGF was funded by the Australian Research Council (ARC) and the University of Queensland. This study was also supported by the ARC Discovery Grant DP130103813 to GFK. EABU would like to acknowledge funding from the University of Queensland (International Postgraduate Research Scholarship, UQ Centennial Scholarship, and UQ Advantage Top-Up Scholarship) and the Norwegian State Education Loans Fund. KS was funded by a PhD grant (SFRH/BD/61959/2009) from F.C.T. (Fundação para a Ciência e a Tecnologia). AA was funded by the project PTDC/AACAMB/121301/2010 (FCOMP-01-0124-FEDER-019490) from F.C.T. CC was supported by the National Science Foundation Graduate Research Fellowship under Grant No. 2012134810 and therefore must include the statement "Any opinion, findings, and conclusions or recommendations expressed in this material are those of the author(s) and do not necessarily reflect the views of the National Science Foundation." We thank Joel Almquist, Erick and Erin Briggs, Aaron Corbit, Karin Greenwood, Heidi and Todd Hoggan, Maximus Kyung Hyun Lee, and Julie King for donating snakes or providing research assistance.

Appendix A. Supplementary data

Supplementary data to this article can be found online at http://dx.doi.org/10.1016/j.jprot.2014.01.013.

REFERENCES

[1] Ali SA, Yang D, Jackson TN, Undheim EA, Koludarov I, Wood K, et al. Venom proteomic characterization and relative antivenom neutralization of two medically important Pakistani elapid snakes (*Bungarus sindanus* and *Naja naja*). J Proteomics 2013;89:15–23.
[2] Boldrini-Franca J, Correa-Netto C, Silva MM, Rodrigues RS, De La Torre P, Perez A, et al. Snake venomics and antivenomics of *Crotalus durissus* subspecies from Brazil: assessment of geographic variation and its implication on snakebite management. J Proteomics 2010;73:1758–76.
[3] Calvete JJ. Antivenomics and venom phenotyping: a marriage of convenience to address the performance and range of clinical use of antivenoms. Toxicon 2010;56:1284–91.
[4] Calvete JJ. Proteomic tools against the neglected pathology of snake bite envenoming. Expert Rev Proteomics 2011;8:739–58.
[5] Calvete JJ, Escolano J, Sanz L. Snake venomics of *Bitis* species reveals large intragenus venom toxin composition variation: application to taxonomy of congeneric taxa. J Proteome Res 2007;6:2732–45.
[6] Calvete JJ, Juarez P, Sanz L. Snake venomics. Strategy and applications. J Mass Spectrom 2007;42:1405–14.
[7] Calvete JJ, Pérez A, Lomonte B, Sánchez EE, Sanz L. Snake venomics of *Crotalus tigris*: the minimalist toxin arsenal of the deadliest Neartic rattlesnake venom. Evolutionary clues for generating a pan-specific antivenom against crotalid type II venoms. J Proteome Res 2012;11:1382–90.
[8] Calvete JJ, Sanz L, Angulo Y, Lomonte B, Gutierrez JM. Venoms, venomics, antivenomics. FEBS Lett 2009;583:1736–43.
[9] Calvete JJ, Sanz L, Cid P, de la Torre P, Flores-Díaz M, Dos Santos MC, et al. Snake venomics of the Central American rattlesnake *Crotalus simus* and the South American *Crotalus durissus* complex points to neurotoxicity as an adaptive paedomorphic trend along *Crotalus* dispersal in South America. J Proteome Res 2009;9:528–44.
[10] Fry BG, Lumsden NG, Wuster W, Wickramaratna JC, Hodgson WC, Kini RM. Isolation of a neurotoxin (alpha-colubritoxin) from a nonvenomous colubrid: evidence for early origin of venom in snakes. J Mol Evol 2003;57:446–52.
[11] Fry BG, Wickramaratna JC, Hodgson WC, Alewood PF, Kini RM, Ho H, et al. Electrospray liquid chromatography/mass spectrometry fingerprinting of *Acanthophis* (death adder) venoms: taxonomic and toxinological implications. Rapid Commun Mass Spectrom 2002;16:600–8.
[12] Fry BG, Wuster W, Ryan Ramjan SF, Jackson T, Martelli P, Kini RM. Analysis of Colubroidea snake venoms by liquid chromatography with mass spectrometry: evolutionary and toxinological implications. Rapid Commun Mass Spectrom 2003;17:2047–62.
[13] Georgieva D, Arni RK, Betzel C. Proteome analysis of snake venom toxins: pharmacological insights. Expert Rev Proteomics 2008;5:787–97.
[14] Gutierrez JM, Lomonte B, Leon G, Alape-Giron A, Flores-Diaz M, Sanz L, et al. Snake venomics and antivenomics: proteomic tools in the design and control of antivenoms for the treatment of snakebite envenoming. J Proteomics 2009;72:165–82.
[15] Gutierrez JM, Sanz L, Escolano J, Fernandez J, Lomonte B, Angulo Y, et al. Snake venomics of the Lesser Antillean pit vipers *Bothrops caribbaeus* and *Bothrops lanceolatus*: correlation with toxicological activities and immunoreactivity of a heterologous antivenom. J Proteome Res 2008;7:4396–408.
[16] Casewell NR, Harrison RA, Wuster W, Wagstaff SC. Comparative venom gland transcriptome surveys of the saw-scaled vipers (Viperidae: *Echis*) reveal substantial intra-family gene diversity and novel venom transcripts. BMC Genomics 2009;10:564.
[17] Ching AT, Rocha MM, Paes Leme AF, Pimenta DC, de Fatima DFM, Serrano SM, et al. Some aspects of the venom proteome of the Colubridae snake *Philodryas olfersii* revealed from a Duvernoy's (venom) gland transcriptome. FEBS Lett 2006;580:4417–22.
[18] Fry BG, Roelants K, Winter K, Hodgson WC, Griesman L, Kwok HF, et al. Novel venom proteins produced by differential domain-expression strategies in beaded lizards and gila monsters (genus *Heloderma*). Mol Biol Evol 2010;27:395–407.
[19] Fry BG, Scheib H, de LMJdA I, Silva DA, Casewell NR. Novel transcripts in the maxillary venom glands of advanced snakes. Toxicon 2012;59:696–708.
[20] Fry BG, Undheim EA, Ali SA, Jackson TN, Debono J, Scheib H, et al. Squeezers and leaf-cutters: differential diversification

and degeneration of the venom system in toxicoferan reptiles. Mol Cell Proteomics 2013;12:1881–99.
[21] Fry BG, Vidal N, Norman JA, Vonk FJ, Scheib H, Ramjan SF, et al. Early evolution of the venom system in lizards and snakes. Nature 2006;439:584–8.
[22] Fry BG, Winter K, Norman JA, Roelants K, Nabuurs RJA, van Osch MJP, et al. Functional and structural diversification of the Anguimorpha lizard venom system. Mol Cell Proteomics 2010;9:2369–90.
[23] Fry BG, Wroe S, Teeuwisse W, van Osch MJ, Moreno K, Ingle J, et al. A central role for venom in predation by *Varanus komodoensis* (Komodo dragon) and the extinct giant *Varanus* (*Megalania*) *priscus*. Proc Natl Acad Sci U S A 2009;106:8969–74.
[24] Rokyta D, Lemmon A, Margres M, Aronow K. The venom-gland transcriptome of the eastern diamondback rattlesnake (*Crotalus adamanteus*). BMC Genomics 2012;13:312.
[25] Rokyta DR, Wray KP, Margres MJ. The genesis of an exceptionally lethal venom in the timber rattlesnake (*Crotalus horridus*) revealed through comparative venom-gland transcriptomics. BMC Genomics 2013;14:394.
[26] Wagstaff SC, Harrison RA. Venom gland EST analysis of the saw-scaled viper, *Echis ocellatus*, reveals novel alpha9beta1 integrin-binding motifs in venom metalloproteinases and a new group of putative toxins, renin-like aspartic proteases. Gene 2006;377:21–32.
[27] Wagstaff SC, Sanz L, Juarez P, Harrison RA, Calvete JJ. Combined snake venomics and venom gland transcriptomic analysis of the ocellated carpet viper, *Echis ocellatus*. J Proteomics 2009;71:609–23.
[28] Anaya M, Rael ED, Lieb CS, Perez JC, Salo RJ. Antibody detection of venom protein variation within a population of the rattlesnake *Crotalus v. viridis*. J Herpetol 1992;26:473–82.
[29] Bush SP, Green SM, Moynihan JA, Hayes WK, Cardwell MD. Crotalidae polyvalent immune fab (ovine) antivenom is efficacious for envenomations by Southern Pacific rattlesnakes (*Crotalus helleri*). Ann Emerg Med 2002;40:619–24.
[30] Casewell NR, Wuster W, Vonk FJ, Harrison RA, Fry BG. Complex cocktails: the evolutionary novelty of venoms. Trends Ecol Evol 2013;28:219–29.
[31] Fry BG, Casewell NR, Wuster W, Vidal N, Young B, Jackson TN. The structural and functional diversification of the Toxicofera reptile venom system. Toxicon 2012;60:434–48.
[32] Mackessy SP, Baxter LM. Bioweapons synthesis and storage: the venom gland of front-fanged snakes. Zool Anz 2006;245:147–59.
[33] Chippaux J-P, Williams V, White J. Snake venom variability: methods of study, results and interpretation. Toxicon 1991;29:1279–303.
[34] Chiszar DA, Walters A, Urbaniak J, Smith HM, Mackessy SP. Discrimination between envenomated and non-envenomated prey by western diamondback rattlesnakes (*Crotalus atrox*): chemosensory consequences of venom. Copeia 1999:640–8.
[35] Heatwole H, Poran NS. Resistances of sympatric and allopatric eels to sea-snake venoms. Copeia 1995:136–47.
[36] Jansa SA, Voss RS. Adaptive evolution of the venom-targeted vWF protein in opossums that eat pitvipers. PLoS One 2011;6.
[37] Massey DJ, Calvete JJ, Sanchez EE, Sanz L, Richards K, Curtis R, et al. Venom variability and envenoming severity outcomes of the *Crotalus scutulatus scutulatus* (Mojave rattlesnake) from Southern Arizona. J Proteomics 2012;75:2576–87.
[38] Owings D, Coss R. Hunting California ground squirrels: constraints and opportunities for Northern Pacific rattlesnakes. In: Hayes WK, Cardwell MD, Beaman KR, Bush SP, editors. Biology of the rattlesnakes. Loma Linda: Loma Linda University Press; 2008. p. 155–68.
[39] Angulo Y, Escolano J, Lomonte B, Gutierrez JM, Sanz L, Calvete JJ. Snake venomics of Central American pitvipers: clues for rationalizing the distinct envenomation profiles of *Atropoides nummifer* and *Atropoides picadoi*. J Proteome Res 2008;7:708–19.
[40] Fry BG, Scheib H, van der Weerd L, Young B, McNaughtan J, Ramjan SF, et al. Evolution of an arsenal: structural and functional diversification of the venom system in the advanced snakes (Caenophidia). MCP 2008;7:215–46.
[41] Lomonte B, Escolano J, Fernandez J, Sanz L, Angulo Y, Gutierrez JM, et al. Snake venomics and antivenomics of the arboreal neotropical pitvipers *Bothriechis lateralis* and *Bothriechis schlegelii*. J Proteome Res 2008;7:2445–57.
[42] Sanz L, Gibbs HL, Mackessy SP, Calvete JJ. Venom proteomes of closely related *Sistrurus* rattlesnakes with divergent diets. J Proteome Res 2006;5:2098–112.
[43] Tashima AK, Sanz L, Camargo AC, Serrano SM, Calvete JJ. Snake venomics of the Brazilian pitvipers *Bothrops cotiara* and *Bothrops fonsecai*. Identification of taxonomy markers. J Proteomics 2008;71:473–85.
[44] van der Weyden L, Hains PG, Broady KW. Characterisation of the biochemical and biological variations from the venom of the death adder species (*Acanthophis antarcticus*, *A. praelongus* and *A. pyrrhus*). Toxicon 2000;38:1703–13.
[45] Castro EN, Lomonte B, Del Carmen Gutiérrez M, Alagón A, Gutiérrez JM. Intraspecies variation in the venom of the rattlesnake *Crotalus simus* from Mexico: different expression of crotoxin results in highly variable toxicity in the venoms of three subspecies. J Proteomics 2013;87:103–21.
[46] Daltry JC, Ponnudurai G, Shin CK, Tan NH, Thorpe RS, Wuster W. Electrophoretic profiles and biological activities: intraspecific variation in the venom of the Malayan pit viper (*Calloselasma rhodostoma*). Toxicon 1996;34:67–79.
[47] Daltry JC, Wuster W, Thorpe RS. Diet and snake venom evolution. Nature 1996;379:537–40.
[48] Forstner M, Hilsenbeck R, Scudday J. Geographic variation in whole venom profiles from the mottled rock rattlesnake (*Crotalus lepidus lepidus*) in Texas. J Herpetol 1997:277–87.
[49] French WJ, Hayes WK, Bush SP, Cardwell MD, Bader JO, Rael ED. Mojave toxin in venom of *Crotalus helleri* (Southern Pacific Rattlesnake): molecular and geographic characterization. Toxicon 2004;44:781–91.
[50] Mackessy SP. Evolutionary trends in venom composition in the Western Rattlesnakes (*Crotalus viridis* sensu lato): toxicity vs. tenderizers. Toxicon 2010;55:1463–74.
[51] Salazar AM, Guerrero B, Cantu B, Cantu E, Rodríguez-Acosta A, Pérez JC, et al. Venom variation in hemostasis of the Southern Pacific rattlesnake (*Crotalus oreganus helleri*): isolation of hellerase. Comp Biochem Physiol C: Toxicol Pharmacol 2009;149:307–16.
[52] Wilkinson JA, Glenn JL, Straight RC, Sites Jr JW. Distribution and genetic variation in venom A and B populations of the Mojave rattlesnake (*Crotalus scutulatus scutulatus*) in Arizona. Herpetol 1991:54–68.
[53] Menezes MC, Furtado MF, Travaglia-Cardoso SR, Camargo AC, Serrano SM. Sex-based individual variation of snake venom proteome among eighteen *Bothrops jararaca* siblings. Toxicon 2006;47:304–12.
[54] Lopez-Lozano JL, de Sousa MV, Ricart CA, Chavez-Olortegui C, Flores Sanchez E, Muniz EG, et al. Ontogenetic variation of metalloproteinases and plasma coagulant activity in venoms of wild *Bothrops atrox* specimens from Amazonian rain forest. Toxicon 2002;40:997–1006.
[55] Mackessy SP. Venom ontogeny in the Pacific rattlesnakes *Crotalus viridis helleri* and *C. v. oreganus*. Copeia 1988:92–101.
[56] Johnson EK, Kardong KV, Ownby CL. Observations on white and yellow venoms from an individual Southern Pacific rattlesnake (*Crotalus viridis helleri*). Toxicon 1987;25:1169–80.

[57] Mebs D. Toxicity in animals. Trends in evolution? Toxicon 2001;39:87–96.
[58] Sasa M. Diet and snake venom evolution: can local selection alone explain intraspecific venom variation? Toxicon 1999;37:249–52 [author reply 53–60].
[59] Aird SD. Ophidian envenomation strategies and the role of purines. Toxicon 2002;40:335–93.
[60] Brust A, Sunagar K, Undheim EA, Vetter I, Yang DC, Casewell NR, et al. Differential evolution and neofunctionalization of snake venom metalloprotease domains. MCP 2013;12:651–63.
[61] Gibbs HL, Mackessy SP. Functional basis of a molecular adaptation: prey-specific toxic effects of venom from *Sistrurus* rattlesnakes. Toxicon 2009;53:672–9.
[62] Pawlak J, Mackessy SP, Fry BG, Bhatia M, Mourier G, Fruchart-Gaillard C, et al. Denmotoxin, a three-finger toxin from the colubrid snake *Boiga dendrophila* (mangrove catsnake) with bird-specific activity. J Biol Chem 2006;281:29030–41.
[63] Sunagar K, Johnson WE, O'Brien SJ, Vasconcelos V, Antunes A. Evolution of CRISPs associated with toxicoferan-reptilian venom and mammalian reproduction. Mol Biol Evol 2012;29:1807–22.
[64] Vidal N, Hedges SB. The phylogeny of squamate reptiles (lizards, snakes, and amphisbaenians) inferred from nine nuclear protein-coding genes. C R Biol 2005;328:1000–8.
[65] Parkinson CL. Molecular systematics and biogeographical history of pitvipers as determined by mitochondrial ribosomal DNA sequences. Copeia 1999:576–86.
[66] Parkinson CL, Campbell JA, Chippindale PT, Schuett G. Multigene phylogenetic analysis of pitvipers, with comments on their biogeography. In: Schuett GW, Hoggren M, Douglas ME, Greene HW, editors. Biology of the vipers. Eagle Mountain Publishing; 2002. p. 93–110.
[67] Klauber LM. Rattlesnakes: their habits, life histories, and influence on mankind. Univ of California Press; 1997.
[68] Knight A, Styer D, Pelikan S, Campbell JA, Densmore LD, Mindell DP. Choosing among hypotheses of rattlesnake phylogeny: a best-fit rate test for DNA sequence data. Syst Biol 1993;42:356–67.
[69] Kraus F, Mink DG, Brown WM. Crotaline intergeneric relationships based on mitochondrial DNA sequence data. Copeia 1996:763–73.
[70] Mackessy S. Venom composition in rattlesnakes: trends and biological significance. In: Hayes WK, Cardwell MD, Beaman KR, Bush SP, editors. The biology of rattlesnakes. Loma Linda: Loma Linda University Press; 2008. p. 495–510.
[71] Pook CE, Wüster W, Thorpe RS. Historical biogeography of the western rattlesnake (Serpentes: Viperidae: *Crotalus viridis*), inferred from mitochondrial DNA sequence information. Mol Phylogenet Evol 2000;15:269–82.
[72] Werman SD. Phylogeny and the evolution of β-neurotoxic phospholipases A2 (PLA2) in the venoms of rattlesnakes, *Crotalus* and *Sistrurus* (Serpentes: Viperidae). In: Hayes WK, Cardwell MD, Beaman KR, Bush SP, editors. The biology of rattlesnakes. Loma Linda: Loma Linda University Press; 2008. p. 511–36.
[73] Schoenherr AA. A natural history of California. Berkeley: University of California Press; 1992.
[74] Jurado JD, Rael ED, Lieb CS, Nakayasu E, Hayes WK, Bush SP, et al. Complement inactivating proteins and intraspecies venom variation in *Crotalus oreganus helleri*. Toxicon 2007;49:339–50.
[75] Wasserberger J, Ordog G, Merkin TE. Southern Pacific Rattlesnake bite: a unique clinical challenge. J Emerg Med 2006;31:263–6.
[76] Vonk FJ, Jackson K, Doley R, Madaras F, Mirtschin PJ, Vidal N. Snake venom: from fieldwork to the clinic: recent insights into snake biology, together with new technology allowing high-throughput screening of venom, bring new hope for drug discovery. Bioessays 2011;33(4):269–79.
[77] Hayes WK, Mackessy SP. Sensationalistic journalism and tales of snakebite: are rattlesnakes rapidly evolving more toxic venom? Wilderness Environ Med 2010;21:35–45.
[78] Edgar RC. MUSCLE: multiple sequence alignment with high accuracy and high throughput. Nucleic Acids Res 2004;32:1792–7.
[79] Guindon S, Dufayard JF, Lefort V, Anisimova M, Hordijk W, Gascuel O. New algorithms and methods to estimate maximum-likelihood phylogenies: assessing the performance of PhyML 3.0. Syst Biol 2010;59:307–21.
[80] Yang Z. PAML 4: phylogenetic analysis by maximum likelihood. Mol Biol Evol 2007;24:1586–91.
[81] Low DH, Sunagar K, Undheim EA, Ali SA, Alagon AC, Ruder T, et al. Dracula's children: molecular evolution of vampire bat venom. J Proteomics 2013;89:95–111.
[82] Murrell B, Wertheim JO, Moola S, Weighill T, Scheffler K, Kosakovsky Pond SL. Detecting individual sites subject to episodic diversifying selection. PLoS Genet 2012;8: e1002764.
[83] Pond SLK, Frost SDW, Muse SV. HyPhy: hypothesis testing using phylogenies. Bioinformatics 2005;21:676–9.
[84] Pond SL, Scheffler K, Gravenor MB, Poon AF, Frost SD. Evolutionary fingerprinting of genes. Mol Biol Evol 2010;27:520–36.
[85] Pond SLK, Murrell B, Fourment M, Frost SD, Delport W, Scheffler K. A random effects branch-site model for detecting episodic diversifying selection. Mol Biol Evol 2011;28:3033–43.
[86] Kelley LA, Sternberg MJ. Protein structure prediction on the Web: a case study using the Phyre server. Nat Protoc 2009;4:363–71.
[87] DeLano WL. The PyMOL molecular graphics system. Scientific D; 2002 [San Carlos, CA].
[88] Armon A, Graur D, Ben-Tal N. ConSurf: an algorithmic tool for the identification of functional regions in proteins by surface mapping of phylogenetic information. J Mol Biol 2001;307:447–63.
[89] Faure G, Xu H, Saul FA. Crystal structure of crotoxin reveals key residues involved in the stability and toxicity of this potent heterodimeric beta-neurotoxin. J Mol Biol 2011;412:176–91.
[90] Guex N, Peitsch MC, Schwede T. Automated comparative protein structure modeling with SWISS-MODEL and Swiss-PdbViewer: a historical perspective. Electrophoresis 2009;30(Suppl. 1):S162–73.
[91] Guex N, Peitsch MC. SWISS-MODEL and the Swiss-PdbViewer: an environment for comparative protein modeling. Electrophoresis 1997;18:2714–23.
[92] Sali A. Comparative protein modeling by satisfaction of spatial restraints. Mol Med Today 1995;1:270–7.
[93] Humphrey W, Dalke A, Schulten K. VMD: visual molecular dynamics. J Mol Graph 1996;14(33-8):27–8.
[94] Baker NA, Sept D, Joseph S, Holst MJ, McCammon JA. Electrostatics of nanosystems: application to microtubules and the ribosome. Proc Natl Acad Sci U S A 2001;98:10037–41.
[95] Matsudaira PT. A practical guide to protein and peptide purification for microsequencing: access online via Elsevier; 1993.
[96] Green SB, Salkind NJ. Using SPSS for Windows and Macintosh: analyzing and understanding data. 4th ed. Upper Saddle River, NJ, USA: Pearson Prentice Hall; 2005.
[97] Revell TK, Hayes WK. Desert iguanas (*Dipsosaurus dorsalis*) sleep less when in close proximity to a rattlesnake predator (*Crotalus cerastes*). J Herpetol 2009;43:29–37.
[98] Cohen J. Statistical power analysis for the behavioral sciences. 2nd ed. Hillsdale, New Jersey, USA: Erlbaum; 1988.

[99] Nakagawa S. A farewell to Bonferroni: the problems of low statistical power and publication bias. Behav Ecol 2004;15:1044–5.
[100] Durban J, Perez A, Sanz L, Gomez A, Bonilla F, Rodriguez S, et al. Integrated "omics" profiling indicates that miRNAs are modulators of the ontogenetic venom composition shift in the Central American rattlesnake, *Crotalus simus simus*. BMC Genomics 2013;14:234.
[101] Glenn JL, Straight R. Mojave rattlesnake *Crotalus scutulatus scutulatus* venom: variation in toxicity with geographical origin. Toxicon 1978;16:81–4.
[102] Glenn JL, Straight RC, Wolfe MC, Hardy DL. Geographical variation in *Crotalus scutulatus scutulatus* (Mojave rattlesnake) venom properties. Toxicon 1983;21:119–30.
[103] Fadel V, Bettendorff P, Herrmann T, de Azevedo Jr WF, Oliveira EB, Yamane T, et al. Automated NMR structure determination and disulfide bond identification of the myotoxin crotamine from *Crotalus durissus terrificus*. Toxicon 2005;46:759–67.
[104] Radis-Baptista G, Kerkis I. Crotamine, a small basic polypeptide myotoxin from rattlesnake venom with cell-penetrating properties. Curr Pharm Des 2011;17:4351–61.
[105] Gopalakrishnakone P, Hawgood BJ, Holbrooke SE, Marsh NA, Santana De Sa S, Tu AT. Sites of action of Mojave toxin isolated from the venom of the Mojave rattlesnake. Br J Pharmacol 1980;69:421–31.
[106] Dugan EA, Hayes WK. Diet and feeding ecology of the red diamond rattlesnake, *Crotalus ruber* (Serpentes: Viperidae). Herpetol 2012;68:203–17.
[107] Peeters HJ. Mammals of California. University of California Press; 2004.
[108] Stebbins RC. A field guide to western reptiles and amphibians. Third Edition. Houghton Mifflin Company; 2003.
[109] Pawlak J, Mackessy SP, Sixberry NM, Stura EA, Le Du MH, Menez R, et al. Irditoxin, a novel covalently linked heterodimeric three-finger toxin with high taxon-specific neurotoxicity. FASEB J 2009;23:534–45.